Scalar-glueball-mediated scale-anomaly dominance of the confining pressure of the pion in holographic QCD

Daisuke Fujii,[1,2,*] Akihiro Iwanaka,[3,2,†] and Mitsuru Tanaka[4,‡]

[1]*Advanced Science Research Center, Japan Atomic Energy Agency (JAEA), Tokai, 319-1195, Japan*
[2]*Research Center for Nuclear Physics, Osaka University, Ibaraki 567-0048, Japan*
[3]*Yukawa Institute for Theoretical Physics, Kyoto University, Kyoto 606-8502, Japan*
[4]*Department of Physics, Nagoya University, Nagoya 464-8602, Japan*

(Received 26 August 2025; accepted 21 October 2025; published 25 November 2025)

In this work, we analyze the energy density and the stress distribution inside the pion derived from gravitational form factors in top-down holographic QCD. In particular, we show that the dominance of the scale anomaly in the confining pressure, previously observed in the instant form for the nucleon, also holds for the pion in the light-front form. Furthermore, we find that in large-N_c QCD described by this approach, the scalar glueball plays a mediating role in transmitting the confining pressure. These findings support the universal role of the scale anomaly in the stability of hadrons.

DOI: 10.1103/2ngy-t5zp

I. INTRODUCTION

Quantum chromodynamics (QCD) possesses classical scale invariance in the chiral limit, but this symmetry is broken at the quantum level due to renormalization effects, giving rise to a scale anomaly. This anomaly appears in the nonvanishing trace of the energy-momentum tensor (EMT). In the forward limit, the hadronic matrix element of the trace corresponds to the invariant mass for hadrons. It is well established that a significant fraction of the hadron mass originates from the anomalous contribution. Understanding the precise role of the scale anomaly in hadron formation is therefore a fundamental issue in hadron physics.

The matrix elements of the EMT in hadrons contain rich information beyond the mass. The corresponding form factors, i.e., gravitational form factors (GFFs), encode internal properties such as energy density, spin, pressure, and shear force distributions. By decomposing the EMT into its trace and traceless components, one can analyze how the scale anomaly contributes to each physical quantity. This framework also allows for the decomposition of hadron mass and spin [1,2]. Notably, the 2018 experimental determination of the proton's pressure distribution [3] has opened a new avenue for exploring the internal mechanical properties of hadrons, stimulating active research from both theoretical [4–50] and experimental [51–60] perspectives.

In this paper, following Ref. [61], we clarify the role of the scale anomaly in the pressure distribution of the pion using the trace-traceless decomposition. In our previous work [62], we computed the GFFs of the pion using a top-down holographic QCD model based on the D4-D8-$\overline{\text{D8}}$ configuration, so-called the Sakai-Sugimoto (SS) model [63,64], which has successfully reproduced the hadron spectrum and form factors in Refs. [63–116]. In the present study, we utilize the results in Ref. [62] to evaluate the energy and stress distributions of the massless pion, focusing on how the scale anomaly governs the pressure profile via the trace-traceless decomposition. We also reconfirm that the EMT matrix element is dominated by three glueball states and newly provide a detailed breakdown of each state's individual contribution, which was not explored in Ref. [62].

In the instant-form formalism, spatial densities defined via three-dimensional Fourier transforms in the Breit frame inevitably depend on the choice of the constant instant time hypersurface. Lorentz boosts alter this surface, introducing ambiguities in defining the density for a given physical state [117,118]. In contrast, the light-front (LF) formalism, defined on constant LF time hypersurfaces, naturally fixes the center-of-mass motion and allows for an unambiguous definition of transverse densities via two-dimensional Fourier transforms [117–126]. This is particularly relevant for systems like the pion, where the Compton wavelength is comparable to its spatial size and relativistic corrections become significant, as discussed in Refs. [117,118]. For such systems, LF transverse densities offer a unique and well-defined description of internal structure.

*Contact author: daisuke@rcnp.osaka-u.ac.jp
†Contact author: akihiro.iwanaka@yukawa.kyoto-u.ac.jp
‡Contact author: tanaka@hken.phys.nagoya-u.ac.jp

Published by the American Physical Society under the terms of the Creative Commons Attribution 4.0 International license. Further distribution of this work must maintain attribution to the author(s) and the published article's title, journal citation, and DOI. Funded by SCOAP³.

In this work, using the holographic QCD approach, we have shown that the scale anomaly generates a negative contribution to the pressure distribution inside the pion, dominated by scalar glueball. Combined with our earlier findings for the nucleon in instant form [61], this implies that scale-anomaly-induced confining pressure is a universal mechanism, common across both forms (instant vs light-front) and hadron types (nucleon vs pion). These results offer valuable guidance for future theoretical and experimental studies of hadronic internal dynamics.

II. SPATIAL DISTRIBUTION FOR PIONS IN LF FORM

The matrix elements of the EMT for pions are characterized by two independent GFFs, $A(t)$ and $D(t)$, and are defined as

$$\langle \pi^a(p')|T^{\mu\nu}(0)|\pi^b(p)\rangle = \delta^{ab}\left[2P^\mu P^\nu A(t) + \frac{1}{2}(\Delta^\mu\Delta^\nu - \eta^{\mu\nu}\Delta^2)D(t)\right], \quad (1)$$

where $P^\mu = (p^\mu + p'^\mu)/2$, $\Delta^\mu = p'^\mu - p^\mu$, $t = \Delta^2$, and m_π is the pion mass. Throughout this paper, we use the mostly plus metric $\eta^{\mu\nu} = \mathrm{diag}(-1,+1,+1,+1)$, and adopt the normalization convention $\langle \vec{p}'|\vec{p}\rangle = 2p^0(2\pi)^3\delta^{(3)}(\vec{p}-\vec{p}')$ with $p^0 = \sqrt{\vec{p}^2 + m_\pi^2}$. Poincaré symmetry requires that $A(0) = 1$ in the forward limit $t = 0$. In contrast, $D(t)$ is unconstrained at $t = 0$. It has been shown [127] that the D-term is negative for stable systems.

In our previous work [62], we computed the pion's GFFs in the chiral limit using a top-down holographic QCD model based on the D4-D8-$\overline{\mathrm{D8}}$ configuration. In the present study, we utilize these GFFs to analyze the spatial distributions of the pion.

It is common to define hadron density distributions as the three-dimensional Fourier transforms of form factors in the Breit frame, evaluated on equal instant time hypersurfaces ($x^0 = \mathrm{const}$) in the instant form. Because form factors are evaluated between plane-wave momentum eigenstates, the resulting spatial densities assume exact momentum localization. These states are completely delocalized in position space, so their Fourier transforms necessarily diverge [117], casting doubt on the physical interpretation of such three-dimensional densities. To address this issue, a wave-packet approach has been proposed, in which the hadron's center-of-mass is localized by smearing the state with a finite-width wave packet [117,118]. This construction reduces to the Fourier transform of form factors in the nonrelativistic limit, while providing a relativistically consistent framework for defining spatial densities. For hadrons such as the pion—whose Compton wavelength is comparable to its spatial extent—these relativistic effects are especially important and cannot be neglected. Moreover, even when the center-of-mass is fixed using wave packets in the instant form, Lorentz boosts mix equal-time hypersurfaces, leaving residual frame dependence in the resulting densities.

To simultaneously address the above issues, we define two-dimensional transverse density distributions on constant LF time hypersurfaces (x^+: const), i.e., on the transverse $x_\perp$ plane, where $x^\pm \equiv (x^0 \pm x^3)/\sqrt{2}$ and $x^i_\perp \equiv (x^1, x^2)$, following Refs. [117–126]. On this hypersurface, the longitudinal (x^-) direction remains delocalized as a plane wave, while the transverse $x_\perp$ plane can be localized using wave packets. This enables spatial distributions to be analyzed with a well-defined physical meaning. Moreover, in the LF formalism, a two-dimensional Galilean subgroup of the Poincaré group emerges, with the longitudinal momentum $P^+ \equiv \int dx^- d^2x_\perp T^{++} = (P^0 + P^3)/\sqrt{2}$ as its central charge. This structure guarantees the complete elimination of contamination from different time slices. Exploiting these advantages, we investigate the two-dimensional density distributions of pions on constant LF time hypersurfaces.

From Refs. [117,120–126], the LF energy and stress distributions are defined as follows:

$$\epsilon_{2\mathrm{D}}(x_\perp) \equiv \int \frac{d^2\Delta_\perp}{(2\pi)^2} e^{-i\vec{\Delta}_\perp\cdot\vec{x}_\perp} \frac{\langle P^+, \vec{\Delta}_\perp/2|T^{++}|P^+, -\vec{\Delta}_\perp/2\rangle}{2P^+} = P^+ \int \frac{d^2\Delta_\perp}{(2\pi)^2} e^{-i\vec{\Delta}_\perp\cdot\vec{x}_\perp} A(t), \quad (2)$$

$$S^{ij}_{2\mathrm{D}}(x_\perp) \equiv \int \frac{d^2\Delta_\perp}{(2\pi)^2} e^{-i\vec{\Delta}_\perp\cdot\vec{x}_\perp} \frac{\langle P^+, \vec{\Delta}_\perp/2|T^{ij}|P^+, -\vec{\Delta}_\perp/2\rangle}{2P^+} = -\frac{1}{4P^+} \int \frac{d^2\Delta_\perp}{(2\pi)^2} e^{-i\vec{\Delta}_\perp\cdot\vec{x}_\perp} (\Delta^i_\perp\Delta^j_\perp - \Delta^2_\perp\delta^{ij}) D(t), \quad (3)$$

with $x_\perp = |\vec{x}_\perp|$, $\vec{\Delta}_\perp = (\Delta^1, \Delta^2)$, and $i, j = 1, 2$. The stress tensor can be expressed using the transverse pressure $p_{2\mathrm{D}}$ and shear force $s_{2\mathrm{D}}$ as

$$S^{ij}_{2\mathrm{D}} = \delta^{ij} p_{2\mathrm{D}} + \left(\frac{x^i_\perp x^j_\perp}{x^2_\perp} - \frac{1}{2}\delta^{ij}\right) s_{2\mathrm{D}}. \quad (4)$$

Decomposing the EMT into its trace $\hat{T}^{\mu\nu} \equiv (g^{\mu\nu}/4)T^\rho{}_\rho$ and traceless components $\overline{T}^{\mu\nu} \equiv T^{\mu\nu} - (g^{\mu\nu}/4)T^\rho{}_\rho$, the pressure can be separated into two parts:

$$p_{2\mathrm{D}} = \bar{p}_{2\mathrm{D}} + \hat{p}_{2\mathrm{D}}, \quad (5)$$

$$\bar{p}_{2D}(x_\perp) = \frac{1}{2P^+}\int \frac{d^2\Delta_\perp}{(2\pi)^2} e^{-i\vec{\Delta}_\perp\cdot\vec{x}_\perp} \times \left[\frac{m_\pi^2}{2}A(t) + \frac{\Delta_\perp^2}{8}(A(t)+D(t))\right],$$

$$\hat{p}_{2D}(x_\perp) = \frac{1}{2P^+}\int \frac{d^2\Delta_\perp}{(2\pi)^2} e^{-i\vec{\Delta}_\perp\cdot\vec{x}_\perp} \times \left[-\frac{m_\pi^2}{2}A(t) - \frac{\Delta_\perp^2}{8}(A(t)+3D(t))\right],$$

where $\hat{p}_{2D}$ corresponds to the contribution from the trace anomaly.

From these distributions, the mass radius $\langle x_\perp^2\rangle_{\rm mass}$ and mechanical radius $\langle x_\perp^2\rangle_{\rm mech}$ are defined as

$$\langle x_\perp^2\rangle_{\rm mass} = \frac{\int d^2x_\perp x_\perp^2 \epsilon_{2D}(x_\perp)}{\int d^2x_\perp \epsilon_{2D}(x_\perp)} = 4\frac{dA(t)}{dt}\bigg|_{t=0}, \tag{6}$$

$$\langle x_\perp^2\rangle_{\rm mech} = \frac{\int d^2x_\perp x_\perp^2 (x_\perp^i x_\perp^j/x_\perp^2) S_{2D}^{ij}(x_\perp)}{\int d^2x_\perp (x_\perp^i x_\perp^j/x_\perp^2) S_{2D}^{ij}(x_\perp)} = \frac{4D(0)}{\int_{-\infty}^0 dt D(t)}, \tag{7}$$

where $(x_\perp^i x_\perp^j/x_\perp^2)S_{2D}^{ij}$ represents the pressure acting in the radial direction.

III. GRAVITATIONAL FROM FACTORS FROM TOP-DOWN HOLOGRAPHIC QCD

In this section, we formulate a method for evaluating the GFFs of the pion within the top-down holographic QCD approach [63,64], by applying the framework previously developed for the nucleon in Ref. [115].

The SS model, employed in this work as a top-down holographic QCD framework, is constructed by embedding N_f D8-branes as probes into the background geometry generated by N_c D4-branes [128]. This geometry corresponds to a ten-dimensional curved spacetime in type IIA supergravity, which is derived from 11-dimensional supergravity (M-theory) through compactification on a doubly Wick-rotated anti-de Sitter space in seven dimensions (AdS_7) black hole background times a four-sphere:

$$ds^2 = \frac{r^2}{L^2}[f(r)d\tau^2 - dx_0^2 + dx_1^2 + dx_2^2 + dx_3^2 + dx_{11}^2] + \frac{L^2}{r^2}\frac{dr^2}{f(r)} + \frac{L^2}{4}d\Omega_4^2, \tag{8}$$

$$f(r) = 1 - \frac{R^6}{r^6}, \qquad R = \frac{L^2 M_{\rm KK}}{3}, \qquad L^3 = 8\pi g_s N_c l_s^3,$$

$$R_{11} = \frac{\lambda}{2\pi N_c M_{\rm KK}}, \qquad \lambda N_c = \frac{L^6 M_{\rm KK}}{32\pi g_s l_s^5} = 216\pi^3\kappa,$$

where $M_{\rm KK}$ denotes the Kaluza-Klein mass scale associated with the τ direction, g_s is the string coupling, l_s is the string length, λ is the 't Hooft coupling, and R_{11} represents the radius of the compactified x_{11} dimension.

The boundary expectation values of the EMT, $\langle T_{\mu\nu}\rangle$, can be obtained by analyzing the asymptotic behavior of the bulk metric perturbations in the background geometry given by Eq. (8). Specifically, the relation is expressed as

$$\int_{x_{11},\tau} \delta g_{\mu\nu} \sim \frac{2\kappa_7^2 L^5}{6}\frac{\langle T_{\mu\nu}\rangle}{r^4} + \cdots, \tag{9}$$

where κ_7^2 is connected to the 11-dimensional gravitational constant through $\kappa_{11}^2 = {\rm Vol}(S^4)\kappa_7^2 = 8\pi^2/3(L/2)^4\kappa_7^2$. To derive this result, one must employ holographic renormalization within the framework of M-theory, as formulated in Ref. [129]. The advantage of working in 11 dimensions lies in the technical simplification of the renormalization procedure.[1]

To obtain the metric fluctuations δg_{MN} induced by the pion field, we solve the linearized Einstein equations in the bulk spacetime. These equations take the form

$$\bar{\mathcal{H}}_{MN} = \mathcal{H}_{MN} - \frac{g_{MN}}{2}\mathcal{H}_P^P = -2\kappa_7^2\mathcal{T}_{MN}, \tag{10}$$

$$\mathcal{H}_{MN} \equiv \nabla^2\delta g_{MN} + \nabla_M\nabla_N\delta g_P^P - \nabla^P(\nabla_M\delta g_{NP} + \nabla_N\delta g_{MP}) - \frac{12}{L^2}\delta g_{MN},$$

where $M,N,P = 0,1,2,3,\tau,r,11$ label the coordinates of the seven-dimensional spacetime obtained after compactifying S^4. From this equation, we derive the conservation law of the bulk EMT, $\nabla^M\mathcal{T}_{MN} = 0$. The source term $\mathcal{T}_{MN}$ represents the EMT of the bulk matter, which, in our analysis, arises solely from the pion field.

To evaluate the bulk EMT $\mathcal{T}_{MN}$, we consider the embedding of D8 branes into the 11-dimensional background and write the D8-brane action as

$$S_{D8} = -\frac{C}{2\pi R_{11} g_s}\int d\tau dx_{11} d^4x dr d\Omega_4 (\delta(\tau) + \delta(\tau - \pi/M_{\rm KK}))\frac{\sqrt{-G_{(11)}}}{\sqrt{G_{\tau\tau}}}\frac{1}{4} \times G^{MN}G^{PQ}{\rm tr}[F_{MP}F_{NQ}] + \cdots, \tag{11}$$

with $C = (64\pi^6 l_s^5)^{-1}$ and the background metric G_{MN} from Eq. (8). The EMT is defined as

$$\mathcal{T}_{MN} \equiv -\frac{2}{\sqrt{-G_{(11)}}}\frac{\delta S_{D8}}{\delta G_{(11)}^{MN}}{\rm Vol}(S^4),$$

[1]Similar methods for nonconformal ten-dimensional backgrounds have also been established [130].

which gives the following expressions:

$$\mathcal{T}_{MN}(\vec{\Delta}, r) \equiv 2\pi R_{11} \int d\tau' \mathcal{T}_{MN}(\tau', \vec{\Delta}, r), \tag{12}$$

$$\begin{aligned}
\mathcal{T}_{\mu\nu}(\vec{\Delta}, r) &= \frac{L^5}{r^5}\frac{\pi^2 C r^2 L^2}{3g_s\sqrt{f(r)}}\mathrm{tr}\Big[F_{\mu\rho}F_{\nu}{}^{\rho} + k(z)^{4/3}M_{\mathrm{KK}}^2 F_{\mu z}F_{\nu z} \\
&\quad - \frac{\eta_{\mu\nu}}{4}(F_{\rho\sigma}F^{\rho\sigma} + 2k(z)^{4/3}M_{\mathrm{KK}}^2 F_{\rho z}F^{\rho}{}_{z})\Big], \\
\mathcal{T}_{11,11}(\vec{\Delta}, r) &= \frac{L^5}{r^5}\frac{\pi^2 C r L^2}{3g_s\sqrt{f(r)}}\mathrm{tr}\left[-\frac{1}{4}F_{\rho\sigma}F^{\rho\sigma} - \frac{k(z)^{4/3}M_{\mathrm{KK}}^2}{2}F_{\rho z}F^{\rho z}\right], \\
\mathcal{T}_{\mu z}(\vec{\Delta}, r) &= \frac{L^5}{r^5}\frac{\pi^2 C r L^2}{3g_s\sqrt{f(r)}}\mathrm{tr}[F_{\mu\rho}F_{z}{}^{\rho}], \\
\mathcal{T}_{zz}(\vec{\Delta}, r) &= \frac{L^5}{r^5}\frac{\pi^2 C r L^2}{3g_s\sqrt{f(r)}}\mathrm{tr}\left[\frac{1}{2}F_{z\rho}F_{z}{}^{\rho} - \frac{1}{4k(z)^{4/3}M_{\mathrm{KK}}^2}F_{\rho\sigma}F^{\rho\sigma}\right],
\end{aligned}$$

where r and z are related via $z = \pm\sqrt{r^6/R^6 - 1}$ for $r \in [R, \infty)$, and $k(z) = 1 + z^2$. In our setup, the pion is treated as the only bulk field generating gravitational perturbations. Then, the gauge field $A_M(x^\nu, z)$ is decomposed as

$$\begin{aligned}
&A_\mu(x^\nu, z) = 0, \qquad A_z(x^\nu, z) = \pi(x^\mu)\phi_0(z), \\
&\phi_0(z) = c_0 k(z)^{-1},
\end{aligned} \tag{13}$$

where $c_0^{-2} = 2M_{\mathrm{KK}}^2\kappa\int dz k(z)\phi_0(z)^2$ ensures normalization [63]. Since the pion field appears as external lines, it is represented by a plane wave with incoming momentum p_ν, as $\pi(x^\nu) = e^{ip_\nu x^\nu}$.

The metric fluctuation $\delta g_{\mu\nu}$ relevant to our analysis is required to be transverse $\Delta^\mu \delta g_{\mu\nu} \sim 0$ near the boundary, because the conservation of the EMT is satisfied. Such a solution can be written as $\delta g_{ij} \sim \delta g_{ij}^{\mathrm{TT}} + \frac{1}{5}(\delta_{ij} - \Delta_i\Delta_j/\vec{\Delta}^2)\delta g_\alpha^\alpha$, where $\delta g_{ij}^{\mathrm{TT}}$ is the transverse-traceless (TT) part with $i, j = 1, 2, 3$ and $\alpha = \mu, 11, \tau$. Furthermore, in the asymptotically AdS boundary ($r \to \infty$) labeled by (x^μ, τ, x^{11}) of M-theory, the six-dimensional traceless condition $\delta g_\alpha^\alpha \sim 0$ is required. Therefore, we only need to solve the TT modes of the Einstein equation under the axial gauge, which are nothing but the QCD glueball spectra. These TT modes consist of 14 independent components, each of which can be assigned a definite spin quantum number [66] (see also Ref. [65]). Since the background spacetime possesses an SO(4) symmetry in the $x^1 - x^3$ and x^{11} directions, the TT modes can be decomposed into irreducible representations of SO(4): a nine-, a four-, and a one-dimensional block. Each of these blocks satisfies the same linearized Einstein equations. Furthermore, by decomposing these under the SO(3) symmetry of the $x^1 - x^3$ spatial directions, the components can be classified according to their spin. Among the 14 TT modes, only three contribute to the matrix element of EMT: the spin-2 and spin-0 components in the nine-dimensional representation of SO(4), denoted as $\mathrm{T}_4(2^{++})$ and $\mathrm{T}_4(0^{++})$, and the spin-0 component in the one-dimensional representation, denoted as $\mathrm{S}_4(0^{++})$.[2] The remaining modes decay more rapidly near the boundary and do not contribute to the matrix element of EMT.[3]

Among the modes that contribute to the matrix element, we select the components that exhibit the same tensor structure as in Eq. (1):

$$\begin{aligned}
\mathcal{O}_D &= +\frac{3}{8}\mathrm{Tr}G^{\mu\nu}G_{\mu\nu} + \cdots \quad [\text{for } \mathrm{T}_4(0^{++})], \\
\mathcal{O}_E &= -\frac{5}{8}\mathrm{Tr}G^{\mu\nu}G_{\mu\nu} + \cdots \quad [\text{for } \mathrm{S}_4(0^{++})],
\end{aligned}$$

so that $\mathcal{O}_D - \mathcal{O}_E = \mathrm{Tr}G^{\mu\nu}G_{\mu\nu}$ identifies the scalar glueball operator in QCD, where $G_{\mu\nu}$ denotes the field strength of the color gauge field at the boundary. Since this linear combination is not an eigenmode on the gravity side, we keep both $\mathrm{T}_4(0^{++})$ and $\mathrm{S}_4(0^{++})$ modes in our analysis. We note that Ref. [96] concludes that the $\mathrm{S}_4(0^{++})$ state is likely a holographic artifact, since its mass is smaller and its decay width larger than those of the lightest scalar glueball in QCD.

[2] $\mathrm{T}_4(0^{++})$ state is the counterpart of the dilaton in the bulk theory, while $\mathrm{S}_4(0^{++})$ state is the lightest glueball state in this model. The latter has a nonzero component along the compact τ direction and is therefore referred to as the exotic scalar state in Ref. [66]. The corresponding boundary gluonic operators are given in Ref. [96] as

[3] Actually, substituting the pion field (13) into Eq. (23), we confirm that $\delta g_{\mu\nu}^{\mathrm{other}}$ falls faster than T_4 and S_4 mode at $r \to \infty$.

$$\delta g^{\mathrm{T}(2)}_{\alpha\beta}|_{r\to\infty} = \frac{2\kappa_7^2 L^5}{6r^4}\begin{pmatrix} 2\vec{\Delta}^2 & 0 & 0 & 0 \\ 0 & \vec{\Delta}^2\delta_{ij} - \Delta_i\Delta_j & 0 & 0 \\ 0 & 0 & 0 & 0 \\ 0 & 0 & 0 & 0 \end{pmatrix} t_2(t), \tag{14}$$

$$\delta g^{\mathrm{T}(0)}_{\alpha\beta}|_{r\to\infty} = \frac{2\kappa_7^2 L^5}{6r^4}\begin{pmatrix} \Delta^2\eta_{\mu\nu} - \Delta_\mu\Delta_\nu & 0 & 0 \\ 0 & -3\Delta^2 & 0 \\ 0 & 0 & 0 \end{pmatrix} t_0(t), \tag{15}$$

$$\delta g^{\mathrm{S}(0)}_{\alpha\beta}|_{r\to\infty} = \frac{2\kappa_7^2 L^5}{6r^4}\begin{pmatrix} \Delta^2\eta_{\mu\nu} - \Delta_\mu\Delta_\nu & 0 & 0 \\ 0 & \Delta^2 & 0 \\ 0 & 0 & -4\Delta^2 \end{pmatrix} s_0(t), \tag{16}$$

where the $\mathrm{T}_4(2^{++})$ mode is traceless in four-dimensional spacetime, while the $\mathrm{T}_4(0^{++})$ mode includes SO(4)-symmetric space components and corresponds to the dilaton in type IIA supergravity. The $\mathrm{S}_4(0^{++})$ mode is the only one that contains a nonzero τ component.

The expectation values of the temporal and spatial components of the EMT can then be written as

$$\begin{aligned}\langle T_{00}\rangle &= \frac{6r^4}{2\kappa_7^2 L^5}(\delta g^{\mathrm{T}(2)}_{00} + \delta g^{\mathrm{T}(0)}_{00} + \delta g^{\mathrm{S}(0)}_{00})|_{r\to\infty} \\ &= (2t_2 - t_0 - s_0)\vec{\Delta}^2,\end{aligned} \tag{17}$$

$$\begin{aligned}\langle T_{ij}\rangle &= \frac{6r^4}{2\kappa_7^2 L^5}(\delta g^{\mathrm{T}(2)}_{ij} + \delta g^{\mathrm{T}(0)}_{ij} + \delta g^{\mathrm{S}(0)}_{ij})|_{r\to\infty} \\ &= (t_2 + t_0 + s_0)(\vec{\Delta}^2\delta_{ij} - \Delta_i\Delta_j).\end{aligned} \tag{18}$$

By decomposing the metric fluctuations as $\delta g_{\mu\nu} = \delta g^{\mathrm{T}(2)}_{\mu\nu} + \delta g^{\mathrm{T}(0)}_{\mu\nu} + \delta g^{\mathrm{S}(0)}_{\mu\nu} + \delta g^{\mathrm{other}}_{\mu\nu}$, the linearized Einstein equations are reduced to the following form:

$$\begin{aligned}&\frac{r^2}{L^2}\left[\frac{1}{L^2 r^5}\partial_r((r^7 - rR^6)\partial_r) - \frac{L^2\Delta^2}{r^2}\right]\frac{L^2}{r^2}\delta g^{\mathrm{T}}_{\mu\nu} = -2\kappa_7^2\mathcal{T}^{\mathrm{T}}_{\mu\nu}, \\ &\frac{r^2}{L^2}\left[\frac{1}{L^2 r^5}\partial_r\left((r^7 - rR^6)\left(\partial_r + \frac{144r^5R^6}{(5r^5 - 2R^6)(r^6 + 2R^6)}\right)\right)\right. \\ &\left. - \frac{L^2\Delta^2}{r^2}\right]\frac{L^2}{r^2}\delta g^{\mathrm{S}(0)}_{\mu\nu}\Big|_{r\to\infty} = -2\kappa_7^2\mathcal{T}^{\mathrm{S}(0)}_{\mu\nu},\end{aligned}$$

where the EMT is decomposed as $\mathcal{T}_{\mu\nu} = \mathcal{T}^{\mathrm{T}}_{\mu\nu} + \mathcal{T}^{\mathrm{S}(0)}_{\mu\nu} + \mathcal{T}^{\mathrm{other}}_{\mu\nu}$ with $\mathcal{T}^{\mathrm{T}}_{\mu\nu} \equiv \mathcal{T}^{\mathrm{T}(2)}_{\mu\nu} + \mathcal{T}^{\mathrm{T}(0)}_{\mu\nu}$. Since $\delta g^{\mathrm{T}(2)}_{\mu\nu}$ and $\delta g^{\mathrm{T}(0)}_{\mu\nu}$ satisfy the same equation, they are treated collectively as $\delta g^{\mathrm{T}}_{\mu\nu}$.

In line with the method described in Ref. [115], each contribution to the EMT can be expressed as

$$2\kappa_7^2\mathcal{T}^{\mathrm{T}}_{\mu\nu} = 2\kappa_7^2\mathcal{T}_{\mu\nu} - 2\kappa_7^2\mathcal{T}^{\mathrm{S}}_{\mu\nu} - 2\kappa_7^2\mathcal{T}^{\mathrm{other}}_{\mu\nu}, \tag{19}$$

$$\begin{aligned}&2\kappa_7^2\mathcal{T}^{\mathrm{S}}_{\mu\nu} \\ &= \frac{r^6 + 2R^6}{4(r^6 - R^6)}\left(\eta_{\mu\nu} - \frac{\Delta_\mu\Delta_\nu}{\Delta^2}\right)\left[\frac{1}{L^4 r^3}\partial_r(r(r^6 - R^6)\partial_r(a+b)\right. \\ &\left. - 3R^6(a+b)) - \Delta^2 b\right],\end{aligned} \tag{20}$$

$$\begin{aligned}&2\kappa_7^2\mathcal{T}^{\mathrm{other}}_{\mu\nu} \\ &= \frac{1}{L^4 r^3}\partial_r\left[\left(\eta_{\mu\nu} - \frac{\Delta_\mu\Delta_\nu}{\Delta^2}\right)r(r^6 - R^6)\partial_r a - 3R^6\eta_{\mu\nu} b\right],\end{aligned} \tag{21}$$

$$\begin{aligned}\partial_r a &= -\frac{3R^6}{(5r^6 - 2R^6)}b + \frac{9r^{11}}{(5r^6 - 2R^6)R^6}2\kappa_7^2\mathcal{T}_{zz}, \\ b &= -i\frac{\Delta^\mu}{\Delta^2}\frac{r^6\sqrt{r^6 - R^6}}{R^9}2\kappa_7^2\mathcal{T}_{\mu z},\end{aligned} \tag{22}$$

with the following ansatz:

$$\begin{aligned}\delta g^{\mathrm{other}}_{\mu\nu}(\vec{\Delta}, r) &= \frac{r^2}{L^2}\frac{\Delta_\mu\Delta_\nu}{\Delta^2}a(r,\Delta), \\ \delta g^{\mathrm{other}}_{11,11}(\vec{\Delta}, r) &= \frac{r^2}{L^2}b(r,\Delta), \\ \delta g^{\mathrm{other}}_{\tau\tau}(\vec{\Delta}, r) &= \frac{r^2 f(r)}{L^2}(-b(r,\Delta)).\end{aligned} \tag{23}$$

We obtain the metric perturbation sourced by the pion field in the bulk via Green's function method as

$$\begin{aligned}\delta g^{\mathrm{T/S}}_{\mu\nu}(\vec{\Delta}, r) \sim \frac{r^2}{L^2}\int dr'\sqrt{-G_{(7)}(r')}G^{\mathrm{T/S}}(\vec{\Delta}, r, r') \\ \times\frac{L^2}{r'^2}2\kappa_7^2\mathcal{T}^{\mathrm{T/S}}_{\mu\nu}(\vec{\Delta}, r'),\end{aligned} \tag{24}$$

where for the S_4 mode, this form holds asymptotically as $r\to\infty$, which is indicated by the symbol $\sim$. Green's function $G^{\mathrm{T/S}}$ is expanded in terms of the complete set $\Psi^{\mathrm{T/S}}_n(r)$ as

$$G^{\mathrm{T/S}}(\vec{\Delta}, r, r') = \sum_{n=1}^{\infty}\frac{\Psi^{\mathrm{T/S}}_n(r)\Psi^{\mathrm{T/S}}_n(r')}{(m^{\mathrm{T/S}}_n)^2 + \vec{\Delta}^2}, \tag{25}$$

where $\Psi^{\mathrm{T/S}}_n(r)$ are solutions to the following eigenvalue problems:

$$\frac{1}{r^3 L^4}\partial_r((r^7 - rR^6)\partial_r\Psi^{\mathrm{T}}_n) = -(m^{\mathrm{T}}_n)^2\Psi^{\mathrm{T}}_n, \tag{26}$$

$$\frac{1}{r^3L^4}\partial_r\left((r^7-rR^6)\left(\partial_r+\frac{144r^5R^6}{(5r^6-2R^6)(r^6+2R^6)}\right)\Psi_n^{\mathrm{S}}\right)=-(m_n^{\mathrm{S}})^2\Psi_n^{\mathrm{S}}, \tag{27}$$

where $m_n^{\mathrm{T/S}}$ denotes the nth glueball mass for the respective modes. These eigenfunctions satisfy the orthonormality and completeness relations:

$$\frac{r^3}{L^3}\sum_{n=1}^{\infty}\Psi_n^{\mathrm{T/S}}(r)\Psi_n^{\mathrm{T/S}}(r')=\delta(r-r'),$$
$$\int_R^{\infty}dr\frac{r^3}{L^3}\Psi_n^{\mathrm{T/S}}(r)\Psi_m^{\mathrm{T/S}}(r)=\delta_{mn}. \tag{28}$$

It is worth noting that, from Eqs. (14)–(16), the dominant sources for the $\mathrm{T}_4(2^{++})$, $\mathrm{T}_4(0^{++})$, and $\mathrm{S}_4(0^{++})$ modes in the bulk are $\mathcal{T}_{\mu\nu}$, $\mathcal{T}_{11,11}$, and $\mathcal{T}_{\tau\tau}$, respectively.[4]

From Eq. (9), the matrix elements of the EMT can be extracted by reading off the coefficients of the $1/r^4$ terms in the metric fluctuations $\delta g_{\mu\nu}^{\mathrm{T/S}}$. The result can be expressed as

$$\langle\pi^a(p')|T_{\mu\nu}|\pi^a(p)\rangle=\langle T_{\mu\nu}^{\mathrm{T}}\rangle+\langle T_{\mu\nu}^{\mathrm{S}}\rangle, \tag{29}$$

$$\langle\pi^a(p')|T_{\mu\nu}^{\mathrm{T/S}}|\pi^a(p)\rangle=\frac{6}{L^{10}}\sum_{n=1}^{\infty}\alpha_n^{\mathrm{T/S}}\int_R^{\infty}dr'\frac{r'^3\Psi^{\mathrm{T/S}}(r')}{\vec{\Delta}^2+(m_n^{\mathrm{T/S}})^2}\mathcal{T}_{\mu\nu}^{\mathrm{T/S}}(\pi,\phi_0;r',\vec{\Delta}),$$

with $\alpha^{\mathrm{T/S}}=(L^4/6)(m_n^{\mathrm{T/S}})^2\int_R^{\infty}drr^3\Psi_n^{\mathrm{T/S}}(r)$.[5] Here, the expression $\mathcal{T}_{\mu\nu}^{\mathrm{T/S}}(\pi,\phi_0;r',\vec{\Delta})$ denotes the bulk EMT evaluated using the pion field Eq. (13). After changing to the z-coordinate, the matrix elements become

$$\langle\pi^a(p')|T_{\mu\nu}|\pi^a(p)\rangle=\frac{1}{L^7}\int_{-\infty}^{\infty}dz\sum_{n=1}^{\infty}\frac{\alpha_n^{\mathrm{T}}\Psi_n^{\mathrm{T}}(r'(z))}{(m_n^{\mathrm{T}})^2+\vec{\Delta}^2}[2P_\mu P_\nu(J(z))+\frac{1}{2}(\Delta_\mu\Delta_\nu-\eta_{\mu\nu}\Delta^2)(-J(z)-J^{\mathrm{S}}(z)-J^{\mathrm{other}}(z))]+\frac{1}{L^7}\int_{-\infty}^{\infty}dz\sum_{n=1}^{\infty}\frac{\alpha_n^{\mathrm{S}}\Psi_n^{\mathrm{S}}(r'(z))}{(m_n^{\mathrm{S}})^2+\vec{\Delta}^2}\left[\frac{1}{2}(\Delta_\mu\Delta_\nu-\eta_{\mu\nu}\Delta^2)J^{\mathrm{S}}(z)\right], \tag{30}$$

where the source $J(z)$, $J^{\mathrm{S}}(z)$, and $J^{\mathrm{other}}(z)$ are given by

$$J(z)=12\kappa(1+z^2)\phi_0(z)^2,$$
$$J^{\mathrm{S}}(z)=9\kappa(1+z^2)(3+z^2)\phi_0(z)\times\left(\frac{5(1+3z^2)}{(3+5z^2)^2}\phi_0(z)+\frac{2(3+8z^2+5z^4)}{z(3+5z^2)^2}\phi_0'(z)\right),$$
$$J^{\mathrm{other}}(z)=\frac{d}{dz}\left(\frac{36\kappa z(1+z^2)^2\phi_0(z)^2}{3+5z^2}\right). \tag{31}$$

By comparing with Eqs. (17) and (18), each glueball mode can be expressed as

$$t_2(t)=\frac{1}{6L^7}\int_{-\infty}^{\infty}dz\sum_{n=1}^{\infty}\frac{\alpha_n^{\mathrm{T}}\Psi_n^{\mathrm{T}}(r')}{(m_n^{\mathrm{T}})^2+\vec{\Delta}^2}J(z), \tag{32}$$

$$t_0(t)=\frac{1}{3L^7}\int_{-\infty}^{\infty}dz\sum_{n=1}^{\infty}\frac{\alpha_n^{\mathrm{T}}\Psi_n^{\mathrm{T}}(r')}{(m_n^{\mathrm{T}})^2+\vec{\Delta}^2}\times\left[J(z)+\frac{3}{2}J^{\mathrm{S}}(z)+\frac{3}{2}J^{\mathrm{other}}(z)\right], \tag{33}$$

$$s_0(t)=-\frac{1}{2L^7}\int_{-\infty}^{\infty}dz\sum_{n=1}^{\infty}\frac{\alpha_n^{\mathrm{S}}\Psi_n^{\mathrm{S}}(r')}{(m_n^{\mathrm{S}})^2+\vec{\Delta}^2}J^{\mathrm{S}}(z). \tag{34}$$

Using these expressions, the GFFs can be identified as

$$A(t)=6t_2, \tag{35}$$

$$D(t)=-2(t_2+t_0+s_0). \tag{36}$$

From these results, we observe that the form factor $A(t)$ is entirely saturated by the tensor glueball $[\mathrm{T}_4(2^{++})]$ contribution, whereas $D(t)$ receives contributions from all three glueball modes.

IV. NUMERICAL RESULTS

We present numerical results for the pion's GFFs and the associated spatial distributions in the chiral limit ($m_\pi=0$).

To evaluate the infinite sums, we perform an expansion in powers of $\vec{\Delta}^2$ as

[4]Although the full $\mathcal{T}_{\tau\tau}$ vanishes due to Eq. (12), the individual S_4 contribution satisfies $\mathcal{T}_{\tau\tau}^{\mathrm{S}}+\mathcal{T}_{\tau\tau}^{\mathrm{other}}=0$, indicating that $\mathcal{T}_{\tau\tau}^{\mathrm{S}}$ alone acts as the source relevant for the propagation of the S_4 mode.

[5]In the axial gauge, the conservation law of the bulk EMT can be written as

$$\partial^\mu\mathcal{T}_{\mu a}=-\frac{1}{L^4}r^3\partial_r(r(r^6-R^6)\mathcal{T}_{ra}),$$
$$\eta^{ab}\mathcal{T}_{ab}=\frac{1}{L^4r^2}(L^4r^3\partial^\mu\mathcal{T}_{\mu r}+r(r^6-R^6)\partial_r\mathcal{T}_{rr}+(8r^6+R^6)\mathcal{T}_{rr})-\frac{r^6(r^6+2R^6)}{(r^6-R^6)^2}\mathcal{T}_{\tau\tau},$$

with $a, b=0, 1, 2, 3, 11$. Using the first line, we derive

$$ik^\mu\mathcal{T}_{\mu\nu}^{\mathrm{T}}=ik^\mu(\mathcal{T}_{\mu\nu}-\mathcal{T}_{\mu\nu}^{\mathrm{S}}-\mathcal{T}_{\mu\nu}^{\mathrm{other}})=0,$$

where $\partial^\mu\mathcal{T}_{\mu\nu}^{\mathrm{S}}$ vanishes by the tensor structure. From these relations, it is then clear that the matrix elements of the four-dimensional EMT are conserved.

$$\frac{6}{L^7}\int_R^\infty dr' \sum_{n=1}^{\infty} \frac{\alpha_n^{\mathrm{T/S}}\Psi_n^{\mathrm{T/S}}(r')}{(m_n^{\mathrm{T/S}})^2+\vec{\Delta}^2} = \sum_{k=0}^{\infty} F_k^{\mathrm{T/S}}(r')(-\vec{\Delta}^2)^k,$$

$$F_k^{\mathrm{T/S}}(r') = \int_R^\infty dr \frac{r^3}{L^3}\sum_{n=0}^{\infty}\frac{\Psi_n^{\mathrm{T/S}}(r)\Psi_n^{\mathrm{T/S}}(r')}{(m_n)^{2k}}. \quad (37)$$

From the eigenvalue equations (27), $F_k^{\mathrm{T/S}}(r)$ obeys the following recursive relations:

$$\frac{1}{r^3L^4}\partial_r((r^7-rR^6)\partial_r F_k^{\mathrm{T}}) = -F_{k-1}^{\mathrm{T}}, \quad (38)$$

$$\frac{1}{r^3L^4}\partial_r\left((r^7-rR^6)\left(\partial_r + \frac{144r^5R^6}{(5r^6-2R^6)(r^6+2R^6)}\right)F_k^{\mathrm{S}}\right) = -F_{k-1}^{\mathrm{S}}, \quad (39)$$

with the normalization $F_0^{\mathrm{T/S}} = 1$ from Eq. (28). The functions $F_{k\neq 0}^{\mathrm{T/S}}(r)$ can be determined iteratively using the boundary conditions $\partial_r F_k^{\mathrm{T/S}}(r)|_{r\to R} = 1$ and $F_k^{\mathrm{T/S}}(r)|_{r\to\infty} = 0$.

We present the GFFs computed by truncating the series in Eq. (37) at $k = 10$ in Fig. 1, along with the results truncated at $k = 8$ and $k = 9$, and, for comparison, the lattice QCD results of Ref. [29]. The parameters are fixed as $\kappa = 0.00745$ and $M_{\mathrm{KK}} = 949$ MeV, determined from the ρ meson mass 776 MeV and the pion decay constant $f_\pi = 92.4$ MeV [64]. While $A(t)$ shows good convergence up to $t \simeq 0.8$ GeV^2 at $k = 10$, $D(t)$ begins to diverge from around $t \sim 0.5$ GeV^2. Since this model is expected to lose validity as t approaches M_{KK}, further extension is not required.

In the top-down holographic QCD, the magnitude of $D(t)$ decreases more rapidly than $A(t)$, in qualitative agreement with lattice QCD [29]. We attribute this difference to the contribution of the S_4 mode to $D(t)$, which is not present in the bottom-up framework of Ref. [68] because that model does not include an S_4 fluctuation sourced by $\mathcal{T}_{\tau\tau}$. Our analysis is performed in the large-N_c and chiral limits, so a deviation from lattice QCD results is expected. In particular, in the large-N_c regime, the exchange of flavor-singlet scalar mesons (e.g., the sigma meson) is suppressed by $1/N_c$, so the GFFs are dominated by scalar glueball exchange. As a result, the pion radius is reduced; i.e., $A(t)$ exhibits a slower falloff. In contrast, $D(t)$ decreases faster than in lattice QCD result, which we attribute to the relatively small mass of the $S_4(0^{++})$ state that contributes only to $D(t)$. As noted in footnote 2, this state has a lower mass and a larger decay width than the lightest scalar glueball in QCD, and may therefore be a holographic artifact.

In addition, Fig. 1 shows fits to the multipole ansatz $F(t) = F(0)/(1+t/\Lambda^2)^m$ with $F(0) = A(0)$ or $D(0)$ for $m = 2, 3, 4$ (dipole, tripole, quadrupole), plotted as curves together with the GFFs results. The corresponding best-fit

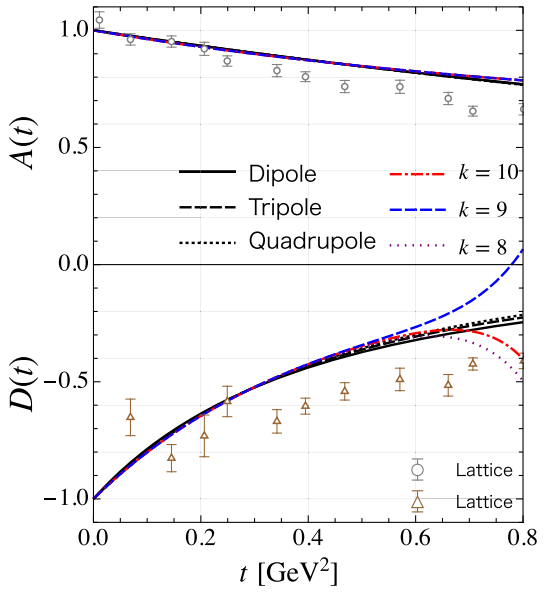


FIG. 1. The pion GFFs $A(t)$ and $D(t)$, shown together with their multipole model fits and the lattice QCD results of Ref. [29].

TABLE I. Multipole-fit parameters Λ^2 for $A(t)$ and $D(t)$ at $m = 2, 3, 4$.

m	Λ^2/GeV^2 for $A(t)$	Λ^2/GeV^2 for $D(t)$
2 (Dipole)	6.36	0.87
3 (Tripole)	9.67	1.38
4 (Quadrupole)	12.98	1.89

values of Λ^2 for $A(t)$ and $D(t)$ at each m are listed in Table I. This multipole ansatz satisfies the following Fourier transform with the modified Bessel function of the second kind K_m:

$$\int \frac{d^2\vec{\Delta}_\perp}{(2\pi)^2}\frac{e^{-i\vec{\Delta}_\perp\cdot\vec{x}_\perp}}{(1+\vec{\Delta}_\perp^2/\Lambda^2)^m} = \frac{\Lambda}{\pi x_\perp}\left(\frac{\Lambda x_\perp}{2}\right)^m \frac{K_{m-1}(\Lambda x_\perp)}{(m-1)!},$$

which provides qualitative insight into how spatial densities behave, following the approach of, e.g., Refs. [122,131].

Using this multipole model, we evaluated the transverse energy density $\epsilon_{2\mathrm{D}}(x_\perp)$, pressure $p_{2\mathrm{D}}(x_\perp)$, and shear force $s_{2\mathrm{D}}(x_\perp)$ based on Eqs. (2)–(4), and present the results in Fig. 2. As seen from these equations, $\epsilon_{2\mathrm{D}}$ is uniquely associated with the tensor glueball, in contrast to $p_{2\mathrm{D}}$ and $s_{2\mathrm{D}}$ which receive contributions from all three glueball modes.

Next, we present in Fig. 3 the decomposition of the pressure based on Eq. (5). Near the center, $\bar{p}_{2\mathrm{D}}$ generates an outward pressure, whereas $\hat{p}_{2\mathrm{D}}$ yields an inward, confining pressure. Although the magnitudes of each contribution are individually large, they mostly cancel each other, resulting in a total pressure whose magnitude is suppressed to

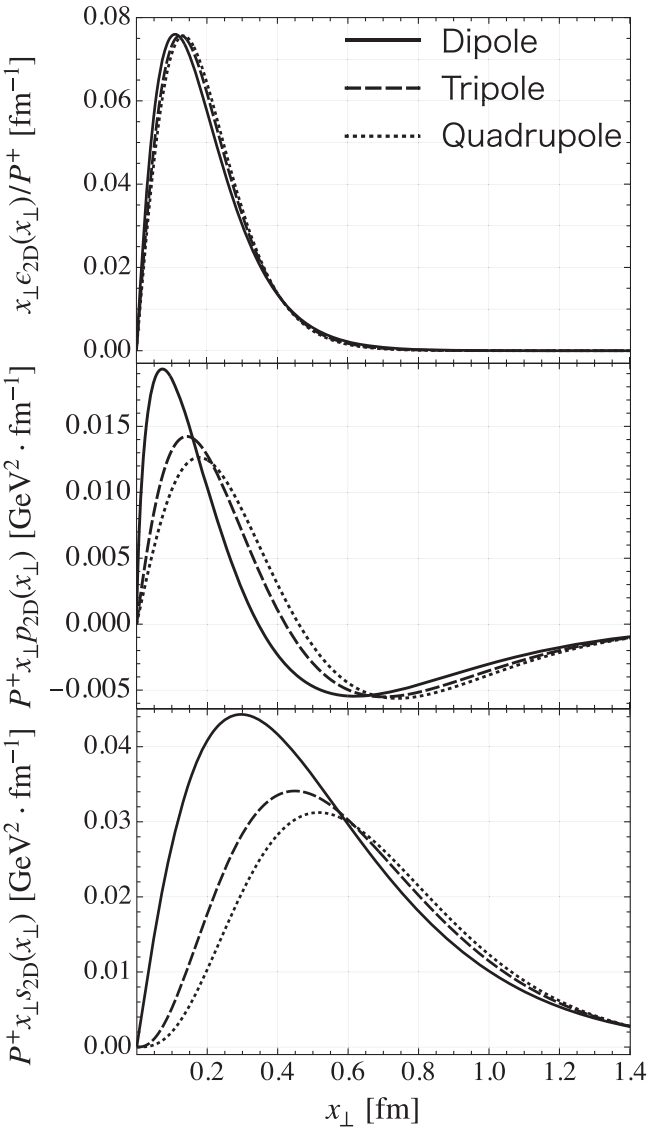


FIG. 2. Energy density $\epsilon_{2D}(x_\perp)$, pressure $p_{2D}(x_\perp)$, and shear force distributions $s_{2D}(x_\perp)$.

roughly $1/10$. In the intermediate region, a sign flip is observed for both $\bar{p}_{2D}$ and $\hat{p}_{2D}$, which is a novel behavior not captured in previous analyses for nucleons in the instant form [61]. In contrast, near the pion surface, the pressure components flip their signs again, and as discussed in Ref. [61], $\hat{p}_{2D}$ induced by the trace anomaly provides a confining pressure. Furthermore, from Eqs. (5), (35), and (36), it is found that the contribution from the $T_4(2^{++})$ mode to the trace anomaly cancels out exactly, indicating that the scalar glueball modes $T_4(0^{++})$ and $S_4(0^{++})$ are responsible for mediating the effects of the trace anomaly.

The fact that the pressure originating from the scale anomaly provides the confining pressure has been confirmed in a model-independent manner in several previous studies [30,48–50]. Furthermore, in the large-N_c limit, the exchange of flavor-singlet scalar mesons is suppressed by

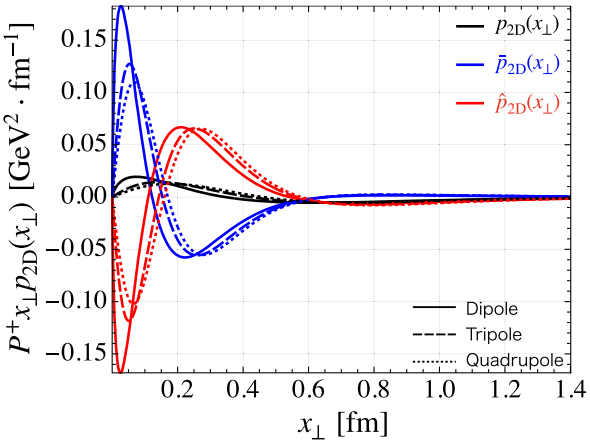


FIG. 3. Pressure decomposition.

$1/N_c$, so the GFFs are dominated by a scalar glueball exchange. This has been discussed in bottom-up holographic QCD for the nucleon [104] and in the instanton liquid model for both the nucleon [132] and the pion [35]. In particular, Refs. [35,132] demonstrate the scalar glueball dominance in the matrix element of the scale anomaly $\langle \hat{T}^{\mu\nu} \rangle$, and confirm that these results are consistent with recent lattice QCD calculations [40]. These studies in the large-N_c limit of QCD support the universality of the phenomenon that we have found in the top-down holographic QCD approach in this paper.

Finally, based on the tripole model fit, we calculate the mass radius $\langle x_\perp^2 \rangle_{\rm mass}$ and the mechanical radius $\langle x_\perp^2 \rangle_{\rm mech}$ as

$$\sqrt{x_{\perp\rm mass}^2} = 0.23 \text{ fm},$$
$$\sqrt{x_{\perp\rm mech}^2} = 0.50 \text{ fm},$$

respectively. As discussed above, within the top-down holographic QCD framework, the former tends to be underestimated while the latter tends to be overestimated.

V. SUMMARY AND OUTLOOKS

In this work, we have investigated the two-dimensional transverse density distributions in the LF form, derived from the GFFs of the pion, using a top-down holographic QCD approach. Following Ref. [61], we performed a trace-traceless decomposition of the EMT to isolate the contribution of the trace anomaly to the pressure distribution. As a result, we have identified the scale-anomaly-driven confining pressure—previously confirmed in the nucleon within the instant form—as also present in the pion on the LF form. The emergence of this same mechanism across distinct dynamical forms (instant vs LF) and hadron types (nucleon vs pion) suggests that the dominance of the scale anomaly in generating confining pressure is a universal

feature of hadron dynamics. Moreover, we found that among the contributing glueball states $T_4(2^{++})$, $T_4(0^{++})$, and $S_4(0^{++})$, the scalar glueballs are responsible for the generation of the confining pressure.

On the other hand, the positive contribution to the pressure induced by the trace anomaly in the intermediate region appears to be a notable feature of the Nambu-Goldstone boson nature of the pion. This is supported by the fact that each component of the pressure decomposition satisfies the von Laue condition individually, i.e., $\int d^2x_\perp \bar{p}_{2D}(x_\perp) = m_\pi^2/4 = 0$ and $\int d^2x_\perp \hat{p}_{2D}(x_\perp) = -m_\pi^2/4 = 0$. It would be of great interest to further explore this characteristic behavior by incorporating current quark mass effects following Refs. [133–139], which we leave for future work. This approach, when applied to different hadrons such as the nucleon, can further clarify which features of the stress distribution are universal and which arise from the intrinsic properties of each hadron.

ACKNOWLEDGMENTS

We are grateful to the authors of Ref. [29] for generously supplying the data tables utilized in Fig. 1. This work was supported in part by the Japan Society for the Promotion of Science (JSPS) KAKENHI (Grants No. JP24K17054 and No. JP24KJ16200) and the COREnet project of RCNP, Osaka University.

DATA AVAILABILITY

The data that support the findings of this article are not publicly available. The data are available from the authors upon reasonable request.

[1] X.-D. Ji, A QCD analysis of the mass structure of the nucleon, Phys. Rev. Lett. **74**, 1071 (1995).
[2] X.-D. Ji, Gauge-invariant decomposition of nucleon spin, Phys. Rev. Lett. **78**, 610 (1997).
[3] V. D. Burkert, L. Elouadrhiri, and F. X. Girod, The pressure distribution inside the proton, Nature (London) **557**, 396 (2018).
[4] M. V. Polyakov and C. Weiss, Skewed and double distributions in pion and nucleon, Phys. Rev. D **60**, 114017 (1999).
[5] D. Brommel, M. Diehl, M. Gockeler, P. Hagler, R. Horsley, D. Pleiter, P. E. L. Rakow, A. Schafer, G. Schierholz, and J. M. Zanotti, Structure of the pion from full lattice QCD, Proc. Sci., LAT2005 (**2006**) 360 [arXiv:hep-lat/0509133].
[6] D. Brommel, Pion structure from the lattice, Ph.D. thesis, Regensburg University, 2007.
[7] P. Hagler *et al.* (LHPC Collaboration), Nucleon generalized parton distributions from full lattice QCD, Phys. Rev. D **77**, 094502 (2008).
[8] W. Broniowski and E. Ruiz Arriola, Gravitational and higher-order form factors of the pion in chiral quark models, Phys. Rev. D **78**, 094011 (2008).
[9] T. Frederico, E. Pace, B. Pasquini, and G. Salme, Pion generalized parton distributions with covariant and light-front constituent quark models, Phys. Rev. D **80**, 054021 (2009).
[10] P. Masjuan, E. Ruiz Arriola, and W. Broniowski, Meson dominance of hadron form factors and large-N_c phenomenology, Phys. Rev. D **87**, 014005 (2013).
[11] Y.-B. Yang, Y. Chen, T. Draper, M. Gong, K.-F. Liu, Z. Liu, and J.-P. Ma, Meson mass decomposition from lattice QCD, Phys. Rev. D **91**, 074516 (2015).
[12] H.-D. Son and H.-C. Kim, Stability of the pion and the pattern of chiral symmetry breaking, Phys. Rev. D **90**, 111901 (2014).
[13] G. Bali, S. Collins, M. Göckeler, R. Rödl, A. Schäfer, and A. Sternbeck, Nucleon generalized form factors from lattice QCD with nearly physical quark masses, Proc. Sci., LATTICE2015 (**2016**) 118 [arXiv:1601.04818].
[14] C. Fanelli, E. Pace, G. Romanelli, G. Salme, and M. Salmistraro, Pion generalized parton distributions within a fully covariant constituent quark model, Eur. Phys. J. C **76**, 253 (2016).
[15] J. Hudson and P. Schweitzer, D term and the structure of pointlike and composed spin-0 particles, Phys. Rev. D **96**, 114013 (2017).
[16] P. E. Shanahan and W. Detmold, Gluon gravitational form factors of the nucleon and the pion from lattice QCD, Phys. Rev. D **99**, 014511 (2019).
[17] C. Alexandrou, M. Constantinou, K. Hadjiyiannakou, K. Jansen, C. Kallidonis, G. Koutsou, and A. Vaquero Avilés-Casco, Nucleon spin structure from lattice QCD, Proc. Sci., DIS2018 (**2018**) 148 [arXiv:1807.11214].
[18] C. Alexandrou *et al.*, Moments of nucleon generalized parton distributions from lattice QCD simulations at physical pion mass, Phys. Rev. D **101**, 034519 (2020).
[19] A. Freese, A. Freese, I. C. Cloët, and I. C. Cloët, Gravitational form factors of light mesons, Phys. Rev. C **100**, 015201 (2019); **105**, 059901(E) (2022).
[20] C. Alexandrou, S. Bacchio, M. Constantinou, J. Finkenrath, K. Hadjiyiannakou, K. Jansen, G. Koutsou, H. Panagopoulos, and G. Spanoudes, Complete flavor decomposition of the spin and momentum fraction of the proton using lattice QCD simulations at physical pion mass, Phys. Rev. D **101**, 094513 (2020).
[21] A. F. Krutov and V. E. Troitsky, Pion gravitational form factors in a relativistic theory of composite particles, Phys. Rev. D **103**, 014029 (2021).
[22] E. Shuryak and I. Zahed, Nonperturbative quark-antiquark interactions in mesonic form factors, Phys. Rev. D **103**, 054028 (2021).

[23] D. A. Pefkou, D. C. Hackett, and P. E. Shanahan, Gluon gravitational structure of hadrons of different spin, Phys. Rev. D **105**, 054509 (2022).
[24] M. Löffler, P. Wein, T. Wurm, S. Weishäupl, D. Jenkins, R. Rödl, A. Schäfer, and L. Walter (RQCD Collaboration), Mellin moments of spin dependent and independent PDFs of the pion and rho meson, Phys. Rev. D **105**, 014505 (2022).
[25] G. F. de Téramond, H. G. Dosch, T. Liu, R. S. Sufian, S. J. Brodsky, and A. Deur (HLFHS Collaboration), Gluon matter distribution in the proton and pion from extended holographic light-front QCD, Phys. Rev. D **104**, 114005 (2021).
[26] K. Raya, Z.-F. Cui, L. Chang, J.-M. Morgado, C. D. Roberts, and J. Rodriguez-Quintero, Revealing pion and kaon structure via generalised parton distributions *, Chin. Phys. C **46**, 013105 (2022).
[27] X.-B. Tong, J.-P. Ma, and F. Yuan, Gluon gravitational form factors at large momentum transfer, Phys. Lett. B **823**, 136751 (2021).
[28] D. C. Hackett, D. A. Pefkou, and P. E. Shanahan, Gravitational form factors of the proton from lattice QCD, Phys. Rev. Lett. **132**, 251904 (2024).
[29] D. C. Hackett, P. R. Oare, D. A. Pefkou, and P. E. Shanahan, Gravitational form factors of the pion from lattice QCD, Phys. Rev. D **108**, 114504 (2023).
[30] K.-F. Liu, Hadrons, superconductor vortices, and cosmological constant, Phys. Lett. B **849**, 138418 (2024).
[31] H. Dutrieux, R. G. Edwards, C. Egerer, J. Karpie, C. Monahan, K. Orginos, A. Radyushkin, D. Richards, E. Romero, and S. Zafeiropoulos (HadStruc Collaboration), Towards unpolarized GPDs from pseudo-distributions, J. High Energy Phys. 08 (2024) 162.
[32] Y.-Z. Xu, M. Ding, K. Raya, C. D. Roberts, J. Rodríguez-Quintero, and S. M. Schmidt, Pion and kaon electromagnetic and gravitational form factors, Eur. Phys. J. C **84**, 191 (2024).
[33] Y. Li and J. P. Vary, Stress inside the pion in holographic light-front QCD, Phys. Rev. D **109**, L051501 (2024).
[34] W. Broniowski and E. Ruiz Arriola, Gravitational form factors of the pion and meson dominance, Phys. Lett. B **859**, 139138 (2024).
[35] W.-Y. Liu, E. Shuryak, C. Weiss, and I. Zahed, Pion gravitational form factors in the QCD instanton vacuum. I, Phys. Rev. D **110**, 054021 (2024).
[36] W.-Y. Liu, E. Shuryak, and I. Zahed, Pion gravitational form factors in the QCD instanton vacuum. II, Phys. Rev. D **110**, 054022 (2024).
[37] T. Hu, X. Cao, S. Xu, Y. Li, X. Zhao, and J. P. Vary, Gravitational form factor D of charmonium from shear stress, Phys. Rev. D **111**, 074031 (2025).
[38] A. F. Krutov and V. E. Troitsky, Step toward estimation of the neutral-hadron size: The gravitational mass radius of $\pi 0$ meson in a relativistic theory of composite particles, Phys. Rev. D **111**, 034034 (2025).
[39] W. Broniowski and E. Ruiz Arriola, Transverse densities of the energy-momentum tensor and the gravitational form factors the pion, Acta Phys. Pol. B **56**, 3 (2025).
[40] B. Wang, F. He, G. Wang, T. Draper, J. Liang, K.-F. Liu, and Y.-B. Yang (χQCD Collaboration), Trace anomaly form factors from lattice QCD, Phys. Rev. D **109**, 094504 (2024).
[41] S. Sugimoto and T. Tsukamoto, Energy-momentum tensor and D-term of baryons in Top-down holographic QCD, arXiv:2503.19492.
[42] Y. Hatta and J. Schoenleber, Sullivan process near threshold and the pion gravitational form factors, Phys. Rev. Lett. **134**, 251901 (2025).
[43] M. Goharipour, H. Hashamipour, H. Fatehi, F. Irani, K. Azizi, and S. V. Goloskokov (MMGPDs Collaboration), Mechanical properties of the nucleon from the generalized parton distributions, Phys. Rev. D **112**, 014016 (2025).
[44] Z. Dehghan, F. Almaksusi, and K. Azizi, Mechanical properties of proton using flavor-decomposed gravitational form factors, J. High Energy Phys. 06 (2025) 025.
[45] M. Goharipour, F. Irani, M. H. Amiri, H. Fatehi, B. Falahi, A. Moradi, and K. Azizi (MMGPDs Collaboration), Can we determine the exact size of the nucleon?: A comprehensive study of different radii, Nucl. Phys. **B1017**, 116962 (2025).
[46] Z. Dehghan and K. Azizi, Mechanical properties of the Ω^- baryon from gravitational form factors, Phys. Rev. D **112**, 054014 (2025).
[47] X.-H. Cao, F.-K. Guo, Q.-Z. Li, B.-W. Wu, and D.-L. Yao, Gravitational form factors of pions, kaons and nucleons from dispersion relations, arXiv:2507.05375.
[48] X. Ji and C. Yang, Momentum flow and forces on quarks in the nucleon, arXiv:2503.01991.
[49] D. Fujii and M. Tanaka, Scale-anomaly-induced binding pressure in hadrons, Phys. Lett. B **870**, 139872 (2025).
[50] X. Ji and C. Yang, A journey of seeking pressures and forces in the nucleon, arXiv:2508.16727.
[51] S. Uehara *et al.* (Belle Collaboration), Measurement of $\gamma\gamma^* \to \pi^0$ transition form factor at Belle, Phys. Rev. D **86**, 092007 (2012).
[52] M. Masuda *et al.* (Belle Collaboration), Study of π^0 pair production in single-tag two-photon collisions, Phys. Rev. D **93**, 032003 (2016).
[53] S. Kumano, Q.-T. Song, and O. V. Teryaev, Hadron tomography by generalized distribution amplitudes in pion-pair production process $\gamma^*\gamma \to \pi^0\pi^0$ and gravitational form factors for pion, Phys. Rev. D **97**, 014020 (2018).
[54] V. D. Burkert, Jefferson lab at 12 GeV: The science program, Annu. Rev. Nucl. Part. Sci. **68**, 405 (2018).
[55] R. Abdul Khalek *et al.*, Science requirements and detector concepts for the electron-ion collider: EIC Yellow Report, Nucl. Phys. **A1026**, 122447 (2022).
[56] D. P. Anderle *et al.*, Electron-ion collider in China, Front. Phys. (Beijing)**16**, 64701 (2021).
[57] B. Duran *et al.*, Determining the gluonic gravitational form factors of the proton, Nature (London) **615**, 813 (2023).
[58] A. F. Krutov and V. E. Troitsky, Relativistic composite-particle theory of the gravitational form factors of the pion: quantitative results, Phys. Rev. D **106**, 054013 (2022).
[59] F. Georges *et al.* (Jefferson Lab Hall A Collaboration), Deeply virtual Compton scattering cross section at high Bjorken xB, Phys. Rev. Lett. **128**, 252002 (2022).
[60] G. Christiaens *et al.* (CLAS Collaboration), First CLAS12 measurement of deeply virtual Compton scattering

beam-spin asymmetries in the extended valence region, Phys. Rev. Lett. **130**, 211902 (2023).
[61] D. Fujii, M. Kawaguchi, and M. Tanaka, Dominance of gluonic scale anomaly in confining pressure inside nucleon and D-term, Phys. Lett. B **866**, 139559 (2025).
[62] D. Fujii, A. Iwanaka, and M. Tanaka, Gravitational form factors of pion from top-down holographic QCD, Phys. Rev. D **110**, L091501 (2024).
[63] T. Sakai and S. Sugimoto, Low energy hadron physics in holographic QCD, Prog. Theor. Phys. **113**, 843 (2005).
[64] T. Sakai and S. Sugimoto, More on a holographic dual of QCD, Prog. Theor. Phys. **114**, 1083 (2005).
[65] N. R. Constable and R. C. Myers, Spin two glueballs, positive energy theorems and the AdS/CFT correspondence, J. High Energy Phys. 10 (1999) 037.
[66] R. C. Brower, S. D. Mathur, and C.-I. Tan, Glueball spectrum for QCD from AdS supergravity duality, Nucl. Phys. **B587**, 249 (2000).
[67] H. Hata, T. Sakai, S. Sugimoto, and S. Yamato, Baryons from instantons in holographic QCD, Prog. Theor. Phys. **117**, 1157 (2007).
[68] Z. Abidin and C. E. Carlson, Gravitational form factors in the axial sector from an AdS/QCD model, Phys. Rev. D **77**, 115021 (2008).
[69] Z. Abidin and C. E. Carlson, Gravitational form factors of vector mesons in an AdS/QCD model, Phys. Rev. D **77**, 095007 (2008).
[70] Z. Abidin and C. E. Carlson, Nucleon electromagnetic and gravitational form factors from holography, Phys. Rev. D **79**, 115003 (2009).
[71] K. Hashimoto, T. Hirayama, and D. K. Hong, Quark mass dependence of hadron spectrum in holographic QCD, Phys. Rev. D **81**, 045016 (2010).
[72] K. Hashimoto, N. Iizuka, T. Ishii, and D. Kadoh, Three-flavor quark mass dependence of baryon spectra in holographic QCD, Phys. Lett. B **691**, 65 (2010).
[73] T. Imoto, T. Sakai, and S. Sugimoto, Mesons as open strings in a holographic dual of QCD, Prog. Theor. Phys. **124**, 263 (2010).
[74] T. Ishii, Toward bound-state approach to strangeness in holographic QCD, Phys. Lett. B **695**, 392 (2011).
[75] Y. Liu and I. Zahed, Heavy baryons and their exotics from instantons in holographic QCD, Phys. Rev. D **95**, 116012 (2017).
[76] Y. Liu and I. Zahed, Heavy and strange holographic baryons, Phys. Rev. D **96**, 056027 (2017).
[77] K. Hashimoto, Y. Matsuo, and T. Morita, Nuclear states and spectra in holographic QCD, J. High Energy Phys. 12 (2019) 001.
[78] Y. Liu, M. A. Nowak, and I. Zahed, Holographic tetraquarks and the newly observed tcc + at lhcb, Phys. Rev. D **105**, 054021 (2022).
[79] T. Nakas and K. S. Rigatos, Fermions and baryons as open-string states from brane junctions, J. High Energy Phys. 12 (2020) 157.
[80] Y. Hayashi, T. Ogino, T. Sakai, and S. Sugimoto, Stringy excited baryons in holographic quantum chromodynamics, Prog. Theor. Exp. Phys. **2020**, 053B04 (2020).
[81] D. Fujii and A. Hosaka, Heavy baryons in holographic QCD with higher dimensional degrees of freedom, Phys. Rev. D **101**, 126008 (2020).
[82] H. Suganuma and K. Hori, Topological objects in holographic QCD, Phys. Scr. **95**, 074014 (2020).
[83] Y. Liu, M. A. Nowak, and I. Zahed, Holographic charm and bottom pentaquarks. I. Mass spectra with spin effects, Phys. Rev. D **104**, 114021 (2021).
[84] Y. Liu, M. A. Nowak, and I. Zahed, Hyperons and Θs+ in holographic QCD, Phys. Rev. D **105**, 114021 (2022).
[85] K. Hashimoto, C.-I. Tan, and S. Terashima, Glueball decay in holographic QCD, Phys. Rev. D **77**, 086001 (2008).
[86] K. Hashimoto, T. Sakai, and S. Sugimoto, Holographic baryons: Static properties and form factors from gauge/string duality, Prog. Theor. Phys. **120**, 1093 (2008).
[87] H. Hata, M. Murata, and S. Yamato, Chiral currents and static properties of nucleons in holographic QCD, Phys. Rev. D **78**, 086006 (2008).
[88] K.-Y. Kim and I. Zahed, Electromagnetic baryon form factors from holographic QCD, J. High Energy Phys. 09 (2008) 007.
[89] H. R. Grigoryan, T. S. H. Lee, and H.-U. Yee, Electromagnetic nucleon-to-delta transition in holographic QCD, Phys. Rev. D **80**, 055006 (2009).
[90] C. A. Ballon Bayona, H. Boschi-Filho, N. R. F. Braga, and M. A. C. Torres, Form factors of vector and axial-vector mesons in holographic D4-D8 model, J. High Energy Phys. 01 (2009) 052.
[91] C. A. B. Bayona, H. Boschi-Filho, N. R. F. Braga, and M. A. C. Torres, Scattering vector mesons in D4 / D8 model, Nucl. Phys. B, Proc. Suppl. **199**, 119 (2010).
[92] C. A. Ballon Bayona, H. Boschi-Filho, N. R. F. Braga, and M. A. C. Torres, Deep inelastic scattering for vector mesons in holographic D4-D8 model, J. High Energy Phys. 10 (2010) 055.
[93] A. Cherman and T. Ishii, Long-distance properties of baryons in the Sakai-Sugimoto model, Phys. Rev. D **86**, 045011 (2012).
[94] C. A. B. Bayona, H. Boschi-Filho, N. R. F. Braga, M. Ihl, and M. A. C. Torres, Generalized baryon form factors and proton structure functions in the Sakai-Sugimoto model, Nucl. Phys. **B866**, 124 (2013).
[95] M. Harada and M. Rho, Integrating holographic vector dominance to hidden local symmetry for the nucleon form factor, Phys. Rev. D **83**, 114040 (2011).
[96] F. Brünner, D. Parganlija, and A. Rebhan, Glueball decay rates in the Witten-Sakai-Sugimoto model, Phys. Rev. D **91**, 106002 (2015); **93**, 109903(E) (2016).
[97] S.-w. Li, Glueball–baryon interactions in holographic QCD, Phys. Lett. B **773**, 142 (2017).
[98] O. C. Druks, P. H. C. Lau, and I. Zahed, Electromagnetic and axial current form factors and spectroscopy of three-flavor holographic baryons, Phys. Rev. D **99**, 054022 (2019).
[99] K. A. Mamo and I. Zahed, Diffractive photoproduction of J/ψ and Υ using holographic QCD: Gravitational form factors and GPD of gluons in the proton, Phys. Rev. D **101**, 086003 (2020).

[100] D. Chakrabarti, C. Mondal, A. Mukherjee, S. Nair, and X. Zhao, Gravitational form factors and mechanical properties of proton in a light-front quark-diquark model, Phys. Rev. D **102**, 113011 (2020).
[101] D. Fujii and A. Hosaka, Decay properties of roper resonance in the holographic QCD, Phys. Rev. D **104**, 014022 (2021).
[102] Y. Liu, M. A. Nowak, and I. Zahed, Holographic charm and bottom pentaquarks. II. Open and hidden decay widths, Phys. Rev. D **104**, 114022 (2021).
[103] Y. Liu, K. A. Mamo, M. A. Nowak, and I. Zahed, Holographic charm and bottom pentaquarks. III. Excitations through photoproduction of heavy mesons, Phys. Rev. D **104**, 114023 (2021).
[104] K. A. Mamo and I. Zahed, Nucleon mass radii and distribution: Holographic QCD, lattice QCD and GlueX data, Phys. Rev. D **103**, 094010 (2021).
[105] A. Iwanaka, D. Fujii, and A. Hosaka, Decay properties of N(1535) in the holographic QCD, Phys. Rev. D **105**, 114057 (2022).
[106] D. Fujii, A. Iwanaka, and A. Hosaka, Electromagnetic transition amplitude for Roper resonance from holographic QCD, Phys. Rev. D **106**, 014010 (2022).
[107] K. A. Mamo and I. Zahed, J/ψ near threshold in holographic QCD: A and D gravitational form factors, Phys. Rev. D **106**, 086004 (2022).
[108] D. Fujii, Dynamical properties of baryon resonances in the holographic QCD, Ph.D. thesis, Osaka University, 2023.
[109] F. Bigazzi and F. Castellani, Resonance contributions to nucleon spin structure in holographic QCD, J. High Energy Phys. 04 (2023) 037.
[110] F. Hechenberger, J. Leutgeb, and A. Rebhan, Radiative meson and glueball decays in the Witten-Sakai-Sugimoto model, Phys. Rev. D **107**, 114020 (2023).
[111] G. Ramalho and M. T. Peña, Electromagnetic transition form factors of baryon resonances, Prog. Part. Nucl. Phys. **136**, 104097 (2024).
[112] M. Allahverdiyeva and S. Mamedov, Vector meson gravitational form factors and generalized parton distributions at finite temperature within the soft-wall AdS/QCD model, Eur. Phys. J. C **83**, 447 (2023).
[113] F. Castellani, Nucleon electric and magnetic polarizabilities in holographic QCD, Phys. Rev. D **110**, 066001 (2024).
[114] F. Hechenberger, J. Leutgeb, and A. Rebhan, Spin-1 glueballs in the Witten-Sakai-Sugimoto model, Phys. Rev. D **109**, 074014 (2024).
[115] M. Fujita, Y. Hatta, S. Sugimoto, and T. Ueda, Nucleon D-term in holographic quantum chromodynamics, Prog. Theor. Exp. Phys. **2022**, 093B06 (2022).
[116] N. Nasibova and X. D. Arsiwalla, Pion phenomenology from the thermal soft-wall model of holographic QCD, arXiv:2505.23455.
[117] G. A. Miller, Defining the proton radius: A unified treatment, Phys. Rev. C **99**, 035202 (2019).
[118] R. L. Jaffe, Ambiguities in the definition of local spatial densities in light hadrons, Phys. Rev. D **103**, 016017 (2021).
[119] M. Burkardt, Impact parameter dependent parton distributions and off forward parton distributions for zeta—> 0, Phys. Rev. D **62**, 071503 (2000); **66**, 119903(E) (2002).
[120] M. Burkardt, Impact parameter space interpretation for generalized parton distributions, Int. J. Mod. Phys. A **18**, 173 (2003).
[121] M. Diehl, Generalized parton distributions in impact parameter space, Eur. Phys. J. C **25**, 223 (2002); **31**, 277(E) (2003).
[122] A. Freese and G. A. Miller, Forces within hadrons on the light front, Phys. Rev. D **103**, 094023 (2021).
[123] A. Freese and G. A. Miller, Unified formalism for electromagnetic and gravitational probes: Densities, Phys. Rev. D **105**, 014003 (2022).
[124] A. Freese and G. A. Miller, Genuine empirical pressure within the proton, Phys. Rev. D **104**, 014024 (2021).
[125] X. Cao, Y. Li, and J. P. Vary, Forces inside a strongly-coupled scalar nucleon, Phys. Rev. D **108**, 056026 (2023).
[126] A. Freese and G. A. Miller, Synchronization effects on rest frame energy and momentum densities in the proton, Phys. Rev. D **108**, 094026 (2023).
[127] I. A. Perevalova, M. V. Polyakov, and P. Schweitzer, On LHCb pentaquarks as a baryon-ψ(2S) bound state: Prediction of isospin-$\frac{3}{2}$ pentaquarks with hidden charm, Phys. Rev. D **94**, 054024 (2016).
[128] E. Witten, Anti-de Sitter space, thermal phase transition, and confinement in gauge theories, Adv. Theor. Math. Phys. **2**, 505 (1998).
[129] S. de Haro, S. N. Solodukhin, and K. Skenderis, Holographic reconstruction of space-time and renormalization in the AdS/CFT correspondence, Commun. Math. Phys. **217**, 595 (2001).
[130] I. Kanitscheider, K. Skenderis, and M. Taylor, Precision holography for non-conformal branes, J. High Energy Phys. 09 (2008) 094.
[131] C. Lorcé, H. Moutarde, and A. P. Trawiński, Revisiting the mechanical properties of the nucleon, Eur. Phys. J. C **79**, 89 (2019).
[132] W.-Y. Liu, E. Shuryak, and I. Zahed, Glue in hadrons at medium resolution and the QCD instanton vacuum, Phys. Rev. D **110**, 054005 (2024).
[133] R. Casero, E. Kiritsis, and A. Paredes, Chiral symmetry breaking as open string tachyon condensation, Nucl. Phys. **B787**, 98 (2007).
[134] K. Hashimoto, T. Hirayama, and A. Miwa, Holographic QCD and pion mass, J. High Energy Phys. 06 (2007) 020.
[135] O. Bergman, S. Seki, and J. Sonnenschein, Quark mass and condensate in HQCD, J. High Energy Phys. 12 (2007) 037.
[136] A. Dhar and P. Nag, Sakai-Sugimoto model, tachyon condensation and chiral symmetry breaking, J. High Energy Phys. 01 (2008) 055.
[137] K. Hashimoto, T. Hirayama, F.-L. Lin, and H.-U. Yee, Quark mass deformation of holographic massless QCD, J. High Energy Phys. 07 (2008) 089.
[138] A. Dhar and P. Nag, Tachyon condensation and quark mass in modified Sakai-Sugimoto model, Phys. Rev. D **78**, 066021 (2008).
[139] R. McNees, R. C. Myers, and A. Sinha, On quark masses in holographic QCD, J. High Energy Phys. 11 (2008) 056.